Available online at www.sciencedirect.com
SCIENCE DIRECT
Journal of Power Sources 142 (2005) 194–199
JOURNAL OF POWER SOURCES
www.elsevier.com/locate/jpowsour

Carbon deposition in an SOFC fueled by tar-laden biomass gas: a thermodynamic analysis

Devinder Singh[a,*], Eduardo Hernández-Pacheco[a], Phillip N. Hutton[b], Nikhil Patel[b], Michael D. Mann[a]

[a] *Department of Chemical Engineering, University of North Dakota, Grand Forks, ND 58202, USA*
[b] *Energy and Environmental Research Center, University of North Dakota, Grand Forks, ND 58202, USA*

Received 9 October 2004; accepted 29 October 2004
Available online 25 December 2004

Abstract

This work presents a thermodynamic analysis of the carbon deposition in a solid oxide fuel cell (SOFC) fueled by a biomass gasifier. Integrated biomass-SOFC units offer considerable benefits in terms of efficiency and fewer emissions. SOFC-based power plants can achieve a system efficiency of 70–80% (including heat utilization) as compared to 30–37% for conventional systems. The fuel from the biomass gasifier can contain considerable amounts of tars depending on the type of gasifier used. These tars can lead to the deposition of carbon at the anode side of SOFCs and affect the performance of the fuel cells. This paper thermodynamically studies the risk of carbon deposition due to the tars present in the feed stream and the effect various parameters like current density, steam, and temperature have on carbon deposition. Since tar is a complex mixture of aromatics, it is represented by a mixture of toluene, naphthalene, phenol, and pyrene. A total of 32 species are considered for the thermodynamic analysis, which is done by the Gibbs energy minimization technique. The carbon deposition is shown to decrease with an increase in current density and becomes zero after a critical current density. Steam in the feed stream also decreases the amount of carbon deposition. With the increase in temperature the amount of carbon first decreases and then increases.

Keywords: Solid oxide fuel cell; Carbon deposition; Tars; Integrated SOFC-biomass gasification system

1. Introduction

Solid oxide fuel cells (SOFCs) are high-temperature fuel cells which operate in the temperature range of 700–1000 °C. The high operating temperature allows internal reforming, promotes rapid kinetics with non-precious materials, and also produces high-quality by-product heat for cogeneration or for use in a bottoming cycle. SOFCs can be a viable option for generating electricity with considerably higher efficiencies than the conventional systems and considerably lower emissions. SOFC-based power plants can achieve a system efficiency of 70–80% (including heat utilization) as compared to 30–37% for conventional systems [1], and the environmental impact is reduced by a factor of 1/300 for air pollution and 1/5 for water pollution when compared to coal-based plants [2]. The fuel for SOFC's can be obtained from the gasification of biomass, which is a renewable form of energy. Various studies discuss these types of systems in detail [3–7]. The Energy & Environmental Research Center at the University of North Dakota designed a thermally integrated biomass-SOFC gasification system. The system uses a modified downdraft gasifier and is designed such that the high energy effluents from the SOFC are recycled to the gasifier for heat recovery, which increases the biomass-to-gas conversion efficiency. Based on preliminary analysis, biomass-to-electricity conversion efficiencies up to 45% (higher heating value), with net efficiencies up to 38%, are expected. The effluent from the biomass gasifier

* Corresponding author. Tel.: +1 701 777 9148.
E-mail addresses: devinder.singh@und.nodak.edu, singhdevinder17@hotmail.com (D. Singh).

0378-7753/$ – see front matter © 2004 Elsevier B.V. All rights reserved.
doi:10.1016/j.jpowsour.2004.10.024

will consist mainly of carbon monoxide (CO), hydrogen (H_2), methane (CH_4), carbon dioxide (CO_2), water (H_2O), nitrogen (N_2), and various light hydrocarbons along with undesirable impurities like dust, tar, ammonia (NH_3), and some other trace contaminants. The amount and the type of tars present depend on factors such as temperature, gasifying agent, equivalence ratio, residence time, and the type of biomass used [8]. Tars, if present in the stream, pose numerous problems, thus reducing performance and increasing maintenance for end-use devices. For optimal performance of the biomass systems, the effect of tars must be minimized.

The various methods available for tar elimination can be classified as physical processes like filters or scrubbers; thermal processes that crack the heavy aromatic hydrocarbons into products like carbon monoxide, hydrogen, or methane; and catalytic processes that operate at much lower temperatures than the thermal processes. Nair et al. [9] discuss tar removal by pulsed corona discharges as an alternative to catalytic and thermal treatment. Depending on where the tars are removed, tar removal methods can also be classified as primary or secondary methods. Primary methods are the measures taken in the gasifier to prevent the formation of tars or convert the tar formed in the gasifier itself, thus eliminating or minimizing the need of secondary methods. Secondary methods are measures taken downstream of the gasifier and include measures like thermal or catalytic cracking of tars, and the use of a cyclone, filter, or scrubber. Devi et al. [8] give a review of the various primary methods for tar elimination in biomass gasification. Most of the tar elimination systems available suffer from disadvantages that may include a compromise on the flexibility of operation of the gasifier, a reduction in thermodynamic efficiency of the gasification process, systems that are expensive and bulky, production of waste streams or concerns about reliability and catalyst lifetime. The decision whether any of the tar removal methods should be used or to what extent tars must be removed from the gas stream for the combined SOFC-gasifier system will depend primarily on the economics and the tolerance limits of SOFCs to tars. For our specific case where the gasifier effluent is to be fed into an SOFC, tars can lead to the deposition of carbon at the active anode sites and hence degradation of the fuel cell performance. Formation of carbon can take place either by methane cracking or Boudouard reaction:

$$CH_4 \Rightarrow C + 2H_2 \quad (1)$$

$$2CO = C + CO_2 \quad (2)$$

The amount of carbon that is deposited at the anode depends on various factors such as steam/carbon ratio, temperature, material of the anode, and current density at which the cell is operating. Carbon deposition decreases with the increase of steam/carbon ratio or with the increase of current density. There are various studies which discuss the carbon deposition in an SOFC with different fuels [10–16]. In this paper we present a thermodynamic analysis of carbon deposition for tar-laden biomass gasifier fuels which will be presented experimentally in the future. Such an analysis can be used as an initial design tool to give an indication of the expected carbon deposition and help decide if any of the tar elimination method is required for an SOFC process and to what extent the gas needs to be purified of the tar content. Sometimes, careful selection of the operating conditions or simple modification of the process can nullify the effect of tars as far as an SOFC is concerned.

2. Thermodynamic calculations

The thermodynamic analysis was done by calculating the equilibrium compositions using the free energy minimization method when extended to condensed phases. In the calculation, no reactions are considered. Only the Gibbs energy of formation of the species considered are required for the calculation. The data for Gibbs energy was obtained in the form of linear correlations [17–19]. The complete procedure is described by Eriksson [20] and illustrated for carbon deposition by Koh et al. [21].

Since tar is a complex mixture of aromatics with significant amounts of poly aromatic hydrocarbons (PAHs), it is represented here by a mixture of compounds. Table 1 gives the typical composition of biomass gasification tars as reported by Milne et al. [22]. Bergman et al. [23] define tars as all organic components having molecular weight higher than benzene and has come up with a classification system based on their behavior. The classification system developed by Bergman et al. [23] is shown in Table 2. For the calculations presented here, the species and composition to represent tars were chosen keeping in mind the tar classification system by Bergman et al. [23] and the typical composition of biomass gasification tar as reported by Milne et al. [22]. To cover the entire range of significant compounds present in tars, they were represented by a mixture of four compounds with each compound representing a specific class of compounds and the composition equal to the composition of that group in actual tars (Table 1). Table 3 gives the species and their amounts that were chosen to represent tars. Calculations were also done by replacing toluene in Table 3 with benzene, which gave lower carbon deposition, equal to the difference in amount of carbon between benzene and toluene. The same

Table 1
Typical composition of biomass gasification tars [22]

Compound	Composition (wt.%)
Benzene	37.9
Toluene	14.3
Other one-ring aromatic hydrocarbons	13.9
Naphthalene	9.6
Other two-ring aromatic hydrocarbons	7.8
Three-ring aromatic hydrocarbons	3.6
Four-ring aromatic hydrocarbons	0.8
Phenolic compounds	4.6
Heterocyclic compounds	6.5
Others	1.0

Table 2
Tar classification system by Bergman et al. [23]

Class	Type	Examples
1	Gas chromatography (GC) undetectable tars	Biomass fragments, heaviest tars
2	Heterocyclic compounds	Phenol, cresol, quinoline, pyridine
3	Aromatics (1 ring)	Toluene, xylene, ethyl benzene
4	Light polyaromatic hydrocarbons (2–3 rings PAH)	Naphthalene, indene, biphenyl, anthracene, fluorine, phenenthrene
5	Heavy polyaromatic hydrocarbons (≥4 rings PAH)	Pyrene, fluoranthene, benzofluoranthene, perylene
6	GC detectable, not identified compounds	Unknown

Table 3
Mixture chosen to represent tars

Compound	Composition (wt.%)
Toluene: representing all the one-ring compounds	65
Naphthalene: representing two-rings compounds	20
Phenol: representing phenolic and other heterocyclic compounds	10
Pyrene: representing three-rings and higher compounds	5

composition (Table 3) was used in all of the calculations presented in this paper.

Thirty-two species including one condensed phase were considered for our calculation. These species are H_2, CO_2, CO, H_2O, CH_4, O_2, N_2, C_7H_8, $C_{10}H_8$, C_6H_6O, $C_{16}H_{10}$, CH_3OH, $C_{(g)}$, C_2, C_3, H, CH, CH_2, CH_3, N, NO, NO_2, N_2O, N_2O_3, C_2H_2, C_2H_4, C_2H_6, CH_2CO, CH_3CHO, HCHO, HCOOH, and $C_{(s)}$.

3. Results and discussions

3.1. Effect of current density

Current density has a significant impact on carbon deposition as it determines the amount of oxygen ions that are available at the anode for reaction. The oxygen supplied at the cathode undergoes reduction to produce oxygen ions which diffuse through the zirconia-based electrolyte to the anode. For the case of complete diffusion, the amount of oxygen available at the anode can be calculated using the Faraday law:

$$N_{O_2}\,(\mathrm{mol/cm^2\,s}) = \frac{i}{4F} \tag{3}$$

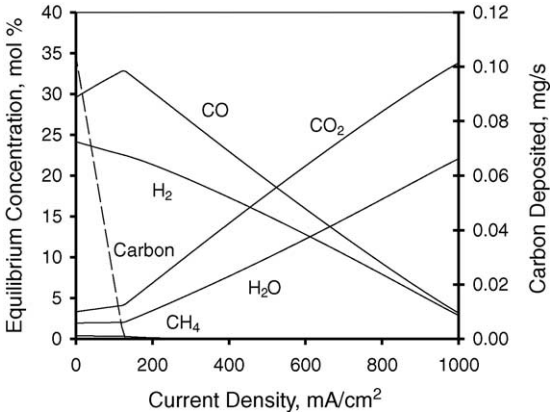

Fig. 1. Equilibrium diagram of main species as a function of current density for a mixture comprising 20% CO, 15% H_2, 10% CO_2, 5% H_2O, 2% CH_4, 48% N_2, and tar as 2% of the total mixture at 750 °C.

where i is the current density in A cm^{-2} and F the Faraday's constant.

For all of the calculations presented here, Eq. (3) was used to calculate the amount of oxygen for a given current density, and the area of the cell was taken to be 16 cm^2. The carbon deposition calculations were done at 750 °C and 150 sccm of the fuel mixture as a function of current density from 0 mA cm^{-2} (open circuit) to 1000 mA cm^{-2}. Fig. 1 shows the equilibrium composition as a function of current density of the main species for a fuel mixture comprising 20% CO, 15% H_2, 10% CO_2, 5% H_2O, 2% CH_4, 48% N_2 on a molar basis, and tar as 2% of the total mixture. The main gas species are shown as mole percent and carbon as (mg s^{-1}) on the second y-axis.

As shown in Fig. 1, the main species were CO, H_2, CO_2, H_2O, and $C_{(s)}$. The amount of $C_{(s)}$ was maximum (0.104 mg s^{-1}) at the open-circuit voltage and decreased with current density because of the possible oxidation of carbon to carbon monoxide and then decreased to zero at a current density of 126 mA cm^{-2}. This current density at which $C_{(s)}$ reduces to zero is known as the threshold current density. Table 4 gives the threshold current density and maximum carbon deposition as a function of tar content. The amount of hydrogen decreases slightly before the threshold current density but decreases abruptly after the threshold current density because of higher electrochemical oxidation of hydrogen to water. The amount of carbon monoxide increases significantly before the threshold current density. The amount of carbon monoxide decreases after the threshold current, and there is a large increase in CO_2 after the threshold current density. Carbon dioxide increases only slightly before the

Table 4
Threshold current density as a function of tar content for a mixture comprising 20% CO, 15% H_2, 10% CO_2, 5% H_2O, 2% CH_4, 48% N_2, and tar as a specified percent of the total mixture at 750 °C

Tar (mol%)	1	2	3	4	5
Threshold current density (mA cm^{-2})	5	126	248	370	492
Maximum carbon deposition (mg s^{-1})	0.004	0.104	0.204	0.305	0.405

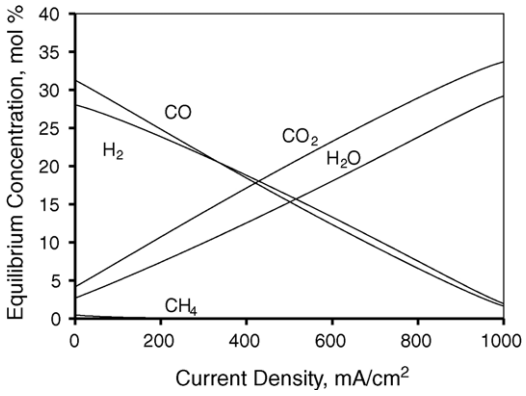

Fig. 2. Equilibrium diagram of main species as a function of current density for a mixture comprising 18% CO, 13% H_2, 10% CO_2, 15% H_2O, 2% CH_4 and 42% N_2 and tar as 2% of the total mixture at 750 °C.

threshold current density. The amount of methane is almost zero for the entire current density range.

3.2. Effect of steam content

To see what effect steam has on carbon deposition equilibrium calculations were done for composition obtained by increasing the moisture content of the mixture to 15%. The feed to the fuel cell comprised 18% CO, 13% H_2, 10% CO_2, 15% H_2O, 2% CH_4 and 42% N_2 on a molar basis, and tars were again 2% of the total feed stream. The equilibrium diagram is shown in Fig. 2. There is no deposition of carbon. The amounts of hydrogen and carbon monoxide decrease through the entire range of current density due to the possible oxidation to water and carbon dioxide, respectively, which increase continuously. The amount of methane is almost zero. The trends are very similar to those in Fig. 1 after the threshold current density. This thermodynamically shows how altering the operating conditions (increasing the steam content) can minimize carbon deposition.

Calculations were also done to obtain the amount of steam that should be present for a given amount of tar to give no carbon deposition. The equilibrium diagram is shown in Fig. 3. As expected, for a given current density, as the steam content increases, the amount of tar that can be present in a feed stream without any risk of carbon deposition increases. For the case of open-circuit voltage, as the amount of tars increase from 2 to 5%, there is a three-fold increase in the amount of steam required to eliminate carbon deposition, from 14.7 to 42.8%.

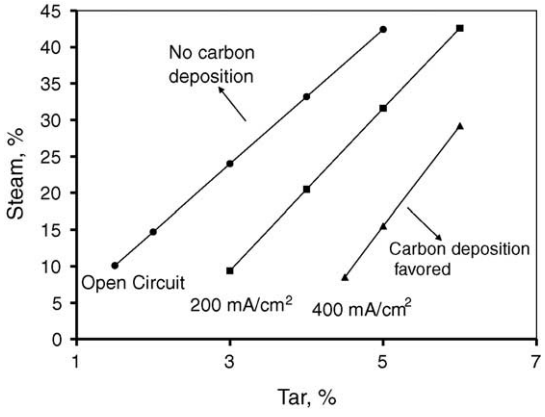

Fig. 3. Equilibrium diagram showing the amount of steam required for a particular tar percentage, to avoid carbon deposition.

3.3. Effect of temperature

The effect of temperature was studied at open-circuit voltage for the same mixture (20% CO, 15% H_2, 10% CO_2, 5% H_2O, 2% CH_4, 48% N_2, and tar as 2% of the total mixture). The temperature was varied from 600 to 1200 °C. The equilibrium diagram with the main species is shown in Fig. 4. As can be seen from the diagram, the carbon deposition initially decreases with temperature up to 920 °C and then increases. The maximum carbon deposition is 0.3 mg s^{-1} at 600 °C and the minimum is 0.04 mg s^{-1} at 920 °C. The temperature range where the carbon deposition is at a minimum corresponds to the upper operating range of SOFCs (800–1000 °C). For explanation purposes, the graph can be divided into two regions, one on the left side of the minimum carbon deposition point (temperature < 920 °C) and the other on the right side (temperature > 920 °C). The amount of carbon dioxide, water, and methane decrease continuously from 600 to 920 °C after which they are almost zero. The amount of carbon monoxide increases rapidly from 600 to 920 °C, and then decreases. The amount of nitrogen is almost constant up to 920 °C and decreases slowly with the increase in nitrogen oxide. The amount of hydrogen increases up to 920 °C and after that becomes almost constant. There is an 87% decrease in carbon from 600 to 920 °C and an increase of 85% from 920 to 1200 °C. Although the actual chemistry is much more complex, the decrease in carbon before 920 °C may be attributed to the oxidation reaction

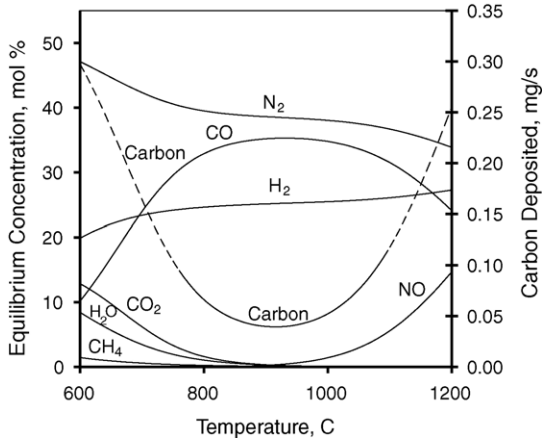

Fig. 4. Equilibrium diagram showing the effect of temperature on carbon deposition for a mixture comprising 20% CO, 15% H_2, 10% CO_2, 5% H_2O, 2% CH_4, 48% N_2 and tar as 2% of the total mixture.

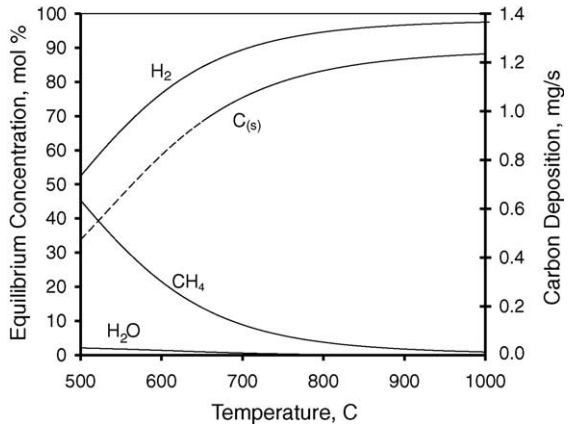

Fig. 5. Equilibrium diagram showing the effect of temperature on carbon deposition for a mixture comprising 97% CH_4 and 3% H_2O.

of carbon to carbon monoxide, which may also explain the rapid increase in carbon monoxide from 600 to 920 °C.

To see what effect composition (like increased water content) has on the carbon deposition behavior, equilibrium calculations were done for a composition with higher amount of water than in the previous case. The trend of all the species was the same except that we had a region of zero carbon deposition in the temperature range corresponding to the upper operating temperature of SOFCs. This carbon deposition behavior with increasing temperature is opposed to that where only methane is used as a fuel. For these types of fuel mixtures which contain mainly methane, carbon deposition increases with temperature and after that becomes constant at a certain maximum level (Fig. 5). This is because for these systems more carbon is formed at a higher temperature possibly because of more methane pyrolysis.

4. Conclusion

The thermodynamic analysis depicted a decrease in the amount of carbon as the current density increased with a threshold value of 126 mA cm^{-2} at the given composition (20% CO, 15% H_2, 10% CO_2, 5% H_2O, 2% CH_4, and 48% N_2) with 2% tar and a temperature of 750 °C. The maximum carbon deposition (0.104 mg s^{-1}) was at the open-circuit voltage. The amount of carbon decreased as the steam content of the fuel stream was increased. Carbon deposition decreased to zero as the operating conditions were varied to get a fuel mixture with higher water content (15%). These variations in the operating conditions can minimize the effect of tars as far as SOFCs are concerned, thus saving on tar removal equipment. The effect of temperature showed that carbon deposition first decreased and then increased as the temperature was increased and that the carbon deposition is around minimum in the upper operating temperature range of SOFCs. Our results showed the conditions at which carbon deposition can be minimized. This type of analysis can be used as an initial design tool to provide an estimate of carbon deposition under various conditions, but a kinetic/experimental study will give a clearer picture.

Acknowledgements

This material is based upon work supported by the National Science Foundation under Grant No. 0093923. We would also like to acknowledge Xcel Energy for its generous support.

References

[1] C. Song, Fuel processing for low-temperature and high-temperature fuel cells. Challenges, and opportunities for sustainable development in the 21st century, Catal. Today 77 (2002) 17–49.
[2] K.L. Seip, B. Thorstensen, H. Wang, Environmental impacts of energy facilities: fuel cell technology compared with coal and conventional gas technology, J. Power Sources 35 (1991) 37–58.
[3] W. Merida, P. Maness, R.C. Brown, D.B. Levi, Enhanced hydrogen production from indirectly heated, gasified biomass, and removal of carbon gas emissions using a novel biological gas reformer, Int. J. Hydrogen Energy 29 (2004) 283–290.
[4] A.O. Omosun, A. Bauen, N.P. Brandon, C.S. Adjiman, D. Hart, Modelling system efficiencies and costs of two biomass-fuelled SOFC systems, J. Power Sources 131 (2004) 96–106.
[5] B. Zhu, X.Y. Bai, G.X. Chen, W.M. Yi, M. Bursell, Fundamental study on biomass-fuelled ceramic fuel cell, Int. J. Energy Res. 26 (2002) 57–66.
[6] T. Makinen, J. Leppalahti, E. Kurtela, Y. Sonatausta, Electricity production from biomass by gasification and solid oxide fuel cell, in: VTT ENERGY, Gasification Research Group Eighth European Conference on Biomass for Energy, Environment, Agriculture and Industry, Vienna, Austria, 1994.
[7] V. Alderucci, P.L. Antonucci, G. Maggio, N. Giordano, V. Antonucci, Thermodynamic analysis of SOFC fuelled by biomass derived gas, Int. J. Hydrogen Energy 19 (4) (1993) 369–376.
[8] L. Devi, K.J. Ptasinski, F.J.J.G. Janssen, A review of the primary measures for tar elimination in biomass gasification processes, Biomass Bioenergy 24 (2003) 125–140.
[9] S.A. Nair, A.J.M. Pemen, K. Yan, F.M. van Gompel, H.E.M. van Leuken, E.J.M. van Heesch, K.J. Ptasinski, A.A.H. Drinkenburg, Tar removal from biomass-derived fuel gas by pulsed corona discharges, Fuel Process. Technol. 84 (2003) 161–173.
[10] S. Park, J.M. Vohs, R.J. Gorte, Direct oxidation of hydrocarbons in a solid-oxide fuel cell, Nature 404 (2000) 265–267.
[11] J.H. Koh, Y.S. Yoo, J. Park, H.C. Lim, Carbon deposition and cell performance of Ni-YSZ anode support SOFC with methane fuel, Solid State Ionics 149 (2002) 157–166.
[12] G.J. Saunders, K. Kendall, Formulating liquid hydrocarbon fuels for SOFCs, in: Electrochemical Society Proceedings, 2003, pp. 1305–1314.
[13] K.M. Walters, A.M. Dean, H. Zhu, R.J. Kee, Homogeneous kinetics and equilibrium predictions of coking propensity in the anode channels of direct oxidation solid-oxide fuel cells using dry natural gas, J. Power Sources 123 (2003) 182–189.
[14] E. Perry Murray, T. Tsai, S.A. Barnett, A direct-methane fuel cell with a ceria-based anode, Nature 400 (1999) 649–651.
[15] T. Takeguchi, Y. Kani, T. Yano, R. Kikuchi, K. Eguchi, K. Tsujimoto, Y. Uchida, A. Ueno, K. Omoshiki, M. Aizawa, Study on steam reforming of CH_4 and C_2 hydrocarbons and carbon de-

position on Ni-YSZ cermets, J. Power Sources 400 (2002) 588–595.
[16] H. Kim, S. Park, J.M. Vohs, R.J. Gorte, Direct oxidation of liquid fuels in a solid oxide fuel cell, J. Electrochem. Soc. 148 (7) (2001) 693–695.
[17] I. Barin, F. Sauert, E. Schultze-Rhonhof, W.S. Sheng, Thermochemical Data of Pure Substances, VCH, Weinheim, 1993.
[18] R.A. Alberty, M.B. Chung, A.K. Reif, Standard chemical thermodynamic properties of polyaromatic hydrocarbons and their isomer groups. ii. Pyrene series, naphthopyrene series, and coronene series, J. Phys. Chem. Ref. Data 18 (1989) 77–109.
[19] C.J. Egan, Heat and free energy of formation of the *cis*- and *trans*-decalins naphthalene and teralin for 298 to 1000 K, J. Chem. Eng. Data 8 (4) (1963) 532–533.
[20] G. Eriksson III, SOLGAS, a computer program for calculating the composition and heat condition of an equilibrium mixture, Acta Chem. Scand. 25 (7) (1971) 2651–2658.
[21] J. Koh, B. Kang, H.C. Lim, Y. Yoo, Thermodynamic analysis of carbon deposition and electrochemical oxidation of methane for SOFC anodes, Electrochem. Solid-State Lett. 4 (2) (2001) A12–A15.
[22] T.A. Milne, N. Abatzoglou, R.J. Evans, Biomass gasifier tars: their nature, formation and conversion, Technical Report NREL/TP-570-25357, National Renewable Energy Laboratory, 1998.
[23] P.C.A. Bergman, S.V.B. van Paasen, H. Boerrigter, The novel "OLGA" technology for complete tar removal from biomass producer gas, in: Pyrolysis and Gasification of Biomass and Waste, Expert Meeting, Strassbourg, France, 2002.